Interaction between magnetic vortex cores in a pair of nonidentical nanodisks

J. P. Sinnecker, H. Vigo-Cotrina, F. Garcia, E. R. P. Novais, and A. P. Guimarães[a)]
Centro Brasileiro de Pesquisas Físicas, 22290-180, Rio de Janeiro, Rio de Janeiro, Brazil

(Received 28 January 2014; accepted 8 May 2014; published online 23 May 2014)

The coupling of two nonidentical magnetic nanodisks, i.e., with different vortex gyrotropic frequencies, is studied. From the analytical approach, the interactions between the nanodisks along x and y directions (the coupling integrals) were obtained as a function of distance. From the numerical solution of Thiele's equation, we derived the eigenfrequencies of the vortex cores as a function of distance. The motion of the two vortex cores and, consequently, the time dependence of the total magnetization M(t) were derived both using Thiele's equation and by micromagnetic simulation. From M(t), a recently developed method, the magnetic vortex echoes, analogous to the Nuclear Magnetic Resonance spin echoes, was used to compute the distance dependence of the magnetic coupling strength. The results of the two approaches differ by approximately 10%; using one single term, a dependence with distance found is broadly in agreement with studies employing other techniques. © *2014 AIP Publishing LLC*. [http://dx.doi.org/10.1063/1.4878875]

I. INTRODUCTION

Magnetic objects of nano- and mesoscopic dimensions of different shapes—squares, ellipses, or disks—may have, as their ground state, a vortex structure.[1–5] This state is characterized by magnetization in the plane of the nanostructure, tangential to concentric circles, and a small core where the magnetization is perpendicular to the plane. One can define the circulation $c = +1$ for counterclockwise (CCW) in-plane magnetization direction, or $c = -1$ for CW direction; the polarity is $p = +1$ for magnetization of the vortex core along the $+z$ axis, and $p = -1$ for the opposite direction ($-z$). The physical description of the vortex properties is usually made within two analytical models: rigid vortex model[6] and the two-vortex ansatz (TVA).[7,8]

Magnetic structures with vortices have many potential applications, e.g., as spin-torque nano-oscillators (STNO's),[9–13] magnetic random memories (MRAM's),[14,15] or logic gates.[16] The applications usually require magnetic elements arranged in a regular array[17,18] where the characterization of the interaction between them is required: in some cases, it is necessary for the functioning of the device; in other cases, it has to be minimized. This interaction allows the coupling of the nanoobjects[19] and the loss-less transmission of energy.[20]

When a magnetic vortex structure—for example, a magnetic nanodisk—is in equilibrium, its vortex core rests at its center, and the structure has magnetic flux-closure. In this configuration, the coupling with nearby nanoelements is minimum. Conversely, when the vortex structure is out of equilibrium, with its core displaced, e.g., by an external magnetic field or a spin-polarized current, magnetostatic coupling with the neighbor elements results. The dependence with distance of this coupling has been the subject of several studies in recent years.[20–23]

Once the excitation of the vortex cores through an external agent is over, they return to their equilibrium position, performing a periodic spiral-like trajectory. This motion, called gyrotropic motion, has been described analytically through Thiele's equation, that is derived from Landau-Lifshitz equation,[24] and has also been obtained from micromagnetic simulations. The angular frequency of this motion depends on the saturation magnetization of the material and on the aspect ratio of the disks. It is typically in the range of hundreds of MHz. Also, several experiments using different techniques have expanded our knowledge of this phenomenon, e.g., Ref. 25.

All these considerations justify why vortex core dynamics, and vortex core interactions, have recently attracted the interest of researchers in the area of Nanomagnetism. Recent studies, both theoretical and experimental, explore the vortex core interaction and vortex dynamics in identical disks pairs.[19–22,26]

The simplest system where one can study interacting nanodisks is, of course, a pair of such magnetic structures; it is, therefore, the ideal system for the investigation of the properties of the interaction, its dependence with distance, etc.

Some devices were proposed using nanodisks with different diameters, e.g., in magnonic devices[27] or in nano-oscillators,[28] although there are few studies of the interactions in more complex structures, such as nonidentical disk arrays in which each element interacts with all the others.[23]

In the present work, the problem of the interaction between pairs of magnetic nanodisks with magnetic vortex structures and different gyrotropic frequencies is analyzed both analytically and through micromagnetic simulation. The present discussion is applicable to pairs of magnetic nanodisks that have different gyrotropic frequencies, arising either from different radii, different materials, or different

a)Author to whom correspondence should be addressed. Electronic mail: apguima@cbpf.br

thicknesses. This may be relevant to the study of fabricated pairs of magnetic nanodisks, where a distribution of frequencies is inherent in the actual samples. We will choose as illustration the difference in radii, as shown in Fig. 1.

Here, we generalized the analytical treatment of the formulation of disk interaction, for any pair of disks. Our results can be well described by interaction intensities that are a multipole expansion with terms of the form d^{-n}, with $n = 3$, 5, 7 and 9, i.e., dipole-dipole, dipole-octupole, octupole-octupole and dipole-triacontadipole interactions, respectively, as recently demonstrated by Sukhostavets *et al.*[18]

Finally, we used the recently reported magnetic vortex echo (MVE) method,[23] in order to obtain information on the interaction between the disks, using the magnetization $M(t)$ given by two different approaches, on the one hand using Thiele's equation, and on another using micromagnetic simulation.

II. RESULTS AND DISCUSSION

A. Analytical description

The analytical description of the interaction between two disks starts by considering both of them with vortex magnetic configuration, and with diameters $2R_1$ and $2R_2$, thickness L and with centers separated by a distance d along the x axis, as shown in Fig. 1. The magnetostatic interaction between the disks is due to the occurrence of magnetic charges σ_i ($i = 1,2$) on their surfaces (top, bottom, and lateral) induced by the shift of the vortex cores from the equilibrium positions.[7] These charges are given in the rigid vortex model by[7,19]

$$\sigma_i = -\frac{c_i M_s (x_i \sin\varphi_i - y_i \cos\varphi_i)}{\sqrt{R_i^2 + |\mathbf{X}_i|^2 - 2R_i(x_i \cos\varphi_i + y_i \sin\varphi_i)}}, \quad (1)$$

where $c_i = \pm 1$ is the ith disk circulation, M_s is saturation magnetization, and $\mathbf{X}_i$, ϕ_i, and R_i are defined according to Fig. 1. The magnetostatic interaction energy $W_{int}(\mathbf{X}_1, \mathbf{X}_2)$ of the side surfaces of two disks is[19,22]

$$W_{int}(\mathbf{X}_1, \mathbf{X}_2) = \frac{1}{2}\int dS_1 \int dS_2 \frac{\sigma_1 \sigma_2}{|\mathbf{r}_1 - \mathbf{r}_2|}. \quad (2)$$

The integration is performed over the surfaces S_1 and S_2 of each disk,[22] $dS_i = R_i dz_i d\varphi_i$, and $\mathbf{r}_1 = \mathbf{r}$, $\mathbf{r}_2 = \mathbf{r}' + d\hat{x}$, as defined by Ref. 22.

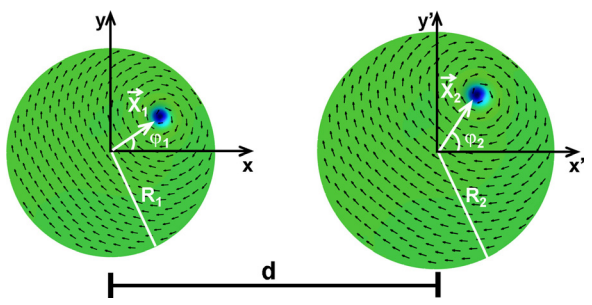

FIG. 1. Coupled disks with vortex magnetic configuration and different radii R_1 and R_2, separated by a center to center distance d.

Inserting Eq. (1) into Eq. (2) and considering $|\mathbf{X}_i|/R \approx 0$ (the vortex displacement is much smaller than the disk radius), we have

$$W_{int}(\mathbf{X}_1, \mathbf{X}_2) = c_1 c_2 (\eta_x x_1 x_2 + \eta_y y_1 y_2) + \mathcal{O}(|X_i|^3), \quad (3)$$

with

$$\eta_{x,y} = \frac{\mu_0 M_s^2 \bar{R}}{8\pi} I_{x,y}, \quad (4)$$

where

$$I_x = \int T \sin\varphi_1 \sin\varphi_2 d\varphi_1 d\varphi_2 d\bar{z}_1 d\bar{z}_2, \quad (5)$$

$$I_y = \int T \cos\varphi_1 \cos\varphi_2 d\varphi_1 d\varphi_2 d\bar{z}_1 d\bar{z}_2, \quad (6)$$

with

$$T = [g_1^2 + g_2^2 + \bar{d}^2 - 2g_1 g_2 \cos(\varphi_2 - \varphi_1) + 2\bar{d}(g_2 \cos\varphi_2 - g_1 \cos\varphi_1) + (\bar{z}_1 + \bar{z}_2)^2]^{-1/2}.$$

Here we have considered the dimensionless variables: $g_i = R_i/\bar{R}$, $\bar{z}_i = z_i/\bar{R}$, $\bar{d} = d/\bar{R}$ with $\bar{R} = (R_1 + R_2)/2$ for $i = 1, 2$.

The limits of integration are from 0 to 2π in ϕ_1, ϕ_2, and from 0 to $L/\bar{R}$ in z_1, z_2.

In Eqs. (5) and (6), I_x and I_y, the coupling integrals, describe the interactions along x and y directions between two disks and can be found by numerical integration. Equations (5) and (6) are a generalization of similar results obtained previously for a pair of coupled identical disks,[19,22] considering now nonidentical disks. Although W_{int} (Eq. (2)) depends on the vortex core polarities,[19] it is worth noting that, in the present approach, the coupling integrals I_x and I_y (Eqs. (5) and (6)) do not.

Fig. 2 shows I_x and I_y calculated for a separation d between the disks in the range $340\,\text{nm} < d < 500\,\text{nm}$.

According to Sukhostavets *et al.*,[18] the interaction between a pair of equal disks can be described using interaction coefficients that depend on the center to center disk distance, as a multipole magnetostatic interaction expansion where the only non-zero terms have odd exponents and the most important interactions to be taken into account for coupled disk dynamics are dipole-dipole, dipole-octupole and octupole-octupole. The coefficients A, B, C, and D are different for interactions along the x and y directions (see Ref. 18, Eq. (16)).

In our results, the interactions in the x and y directions are given by the coupling integrals I_x and I_y, respectively; the difference between these integrals arises naturally, from the symmetry of the problem. The interaction is a function of the distance between the disks, as can be seen in Fig. 2. As the distance increases, I_x and I_y decrease.

The coupling integrals I_x and I_y, when fitted to a single term of the form $\bar{d}^{-n}$, lead to values of $n = 3.41 \pm 0.02$ and $n = 4.08 \pm 0.07$, for I_x and I_y, respectively. These values of n are similar to those found by Sukhostavets *et al.*[18] and Garcia *et al.*[23] for equivalent parameters.

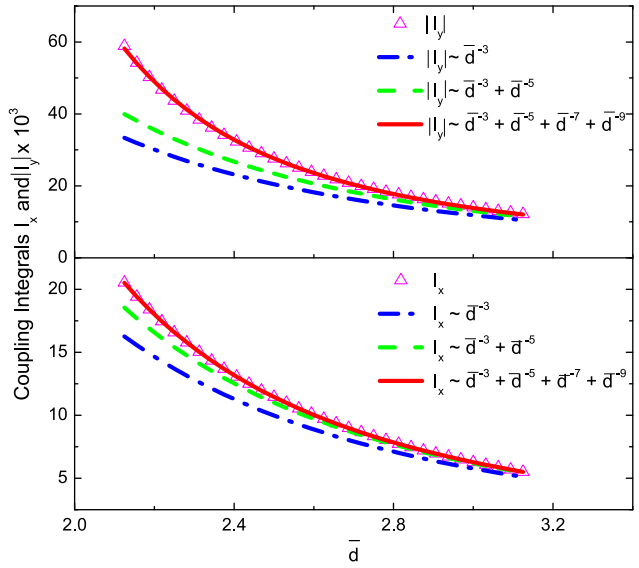

FIG. 2. Coupling integrals I_x and $|I_y|$ as a function of the reduced distance $\bar{d} = d/\bar{R}$ for disks with $L = 20$ nm and $R_1 = 150$ nm and $R_2 = 170$ nm calculated for $340\,\text{nm} < d < 500\,\text{nm}$; the red continuous line is the best fit to a multipole expansion with terms up to $n = 9$; the green dashed line represents the result of a multipole expansion, but considering only the dipolar-dipolar and dipolar-octupolar contributions; the blue dash-dot line is the result of a multipole expansion, considering only the dipolar-dipolar term.

For a smaller distance d, between 340 and 370 nm, we have $n = 3.70 \pm 0.02$ and $n = 5.05 \pm 0.09$ for I_x and I_y, respectively. As the disk distance becomes smaller, the interaction increases and higher-order interaction terms such as dipole-octupole, octupole-octupole terms have a higher contribution, increasing the value of n, as recently obtained[18] for identical disks.

The dependence of I_x and I_y on $\bar{d}$ in Fig. 2 can also be described with a multipole expansion with odd terms of the reduced distance $\bar{d}$ between the disk centers as

$$I_{x,y} = A\bar{d}^{-3} + B\bar{d}^{-5} + C\bar{d}^{-7} + D\bar{d}^{-9}, \tag{7}$$

where the terms of form $\bar{d}^{-n}$, with $n = 3, 5, 7$, and 9 are again the dipole-dipole, dipole-octupole, octupole-octupole and dipole-triacontadipole interactions, respectively.[18]

A good fit can be found when considering all terms, as can be observed in the red continuous line of Fig. 2. For this case, we find values of $A = 156.0 \pm 0.3$, $B = 99 \pm 3$, $C \approx 0$, $D = (1.74 \pm 0.03) \times 10^3$ for I_x and $A = 320 \pm 1$, $B = 286 \pm 10$, $C \approx 0$, $D = (1.6 \pm 0.3) \times 10^3$ for I_y. We can estimate the relevance of each term in Eq. (7) by plotting the curves obtained using the coefficients from the multipole expansion best fit, but considering only the dipole-dipole interaction term (dash-dot blue line in Fig. 2) or the dipole-dipole plus dipole-octupole terms (dashed green line in Fig. 2). By considering only the dipole-dipole interaction $(A\bar{d}^{-3})$, especially for close disks $(d \leq 350\,\text{nm})$, the obtained curve does not describe well the simulation points.

B. Numerical solution of Thiele's equation

One interesting aspect of the coupled nanodisk pair studies is the determination of the vortex gyrotropic eigenfrequencies. These frequencies can be determined analytically using the linearized Thiele's equation, that can be written, considering zero damping[29]

$$\mathbf{G}_i \times \frac{d\mathbf{X}_i}{dt} - \frac{\partial W(\mathbf{X}_1, \mathbf{X}_2)}{\partial \mathbf{X}_i} = 0, \tag{8}$$

where $\mathbf{G}_i$ is the gyrovector, $\mathbf{G}_i = -G_i p_i \hat{z}$, $G_i = 2\pi\mu_0 M_s L_i/\gamma$, γ is the gyromagnetic ratio and M_s is the saturation magnetization.

The potential energy is

$$\begin{aligned} W(\mathbf{X}_1, \mathbf{X}_2) = & W_1(\mathbf{X}_1) \\ & + W_2(\mathbf{X}_2) \\ & + W_{int}(\mathbf{X}_1, \mathbf{X}_2), \end{aligned}$$

where $W_1(\mathbf{X}_1)$ and $W_2(\mathbf{X}_2)$ are the potential energies of each isolated disk. $W_i(\mathbf{X}_i) = W_i(0) + \kappa_i \mathbf{X}_i^2/2$, where $W(0)$ is the potential energy for $\mathbf{X}_i = (0,0)$ and $\kappa_i = 40\pi M_s^2 L_i^2/9R_i$ is the stiffness coefficient.[7] $W_{int}(\mathbf{X}_1, \mathbf{X}_2)$ is the magnetostatic interaction between the disks.

The system of Thiele's equation of motion (Eq. (8)) is simplified using a solution $\mathbf{X}_i(t) = \mathbf{X}_i(\omega)\exp(i\omega t)$, where ω is the frequency, thereby obtaining a matrix equation of the form $\hat{B}\mathbf{A} = i\omega\mathbf{A}$

$$\begin{bmatrix} 0 & -\omega_1 p_1 & 0 & -b\omega_1 p_1 \\ \omega_1 p_1 & 0 & a\omega_1 p_1 & 0 \\ 0 & -d\omega_2 p_2 & 0 & -\omega_2 p_2 \\ c\omega_2 p_2 & 0 & \omega_2 p_2 & 0 \end{bmatrix} \begin{bmatrix} x_1 \\ y_1 \\ x_2 \\ y_2 \end{bmatrix} = i\omega \begin{bmatrix} x_1 \\ y_1 \\ x_2 \\ y_2 \end{bmatrix}, \tag{9}$$

where $a = c_1 c_2 \eta_x / G\omega_1$, $b = c_1 c_2 \eta_y / G\omega_1$, $c = c_1 c_2 \eta_x / G\omega_2$, and $d = c_1 c_2 \eta_y / G\omega_2$ with the eigenfrequency of each isolated disk $\omega_i = \kappa_i / G_i$ (i = 1,2).

From Eq. (9), we get the coupling frequencies ω_i

$$(\omega^p_{+,-})^2 = \frac{{\omega_1}^2 + {\omega_2}^2 + 2bcp\omega_1\omega_2 \pm \sqrt{\triangle}}{2}, \tag{10}$$

where

$$\begin{aligned} \triangle = & ({\omega_1}^2 - {\omega_2}^2)^2 + 4{\omega_1}^2{\omega_2}^2(ca + bd) \\ & + 4p\omega_1\omega_2 bc({\omega_1}^2 + {\omega_2}^2), \end{aligned}$$

with $p = p_1 p_2$; note that in this expression, the circulations c_1 and c_2 only appear squared, and, therefore, the frequencies do not depend on the sign of the circulations c_i.

We considered a disk pair with radii $R_1 = 150$ nm, $R_2 = 170$ nm, and thickness 20 nm separated by a minimum distance $d = 340$ nm, for combined polarities, $p = p_1\, p_2 = +1$ and $p = -1$. The eigenfrequencies of these disks are $\omega_0/2\pi = 0.56$ GHz for $R = 150$ nm and $\omega_0/2\pi = 0.49$ GHz for $R = 170$ nm and were obtained using the two-vortex model.[7,8] These values are in good agreement with those obtained from micromagnetic simulation, respectively, $\omega_0/2\pi = 0.58$ GHz and $\omega_0/2\pi = 0.52$ GHz. However, the eigenfrequencies spread $\Delta\omega$ obtained analytically is larger than the one obtained by the micromagnetic simulation. The

eigenfrequencies of the interacting pair as a function of distance are shown in Fig. 3. It is apparent that for increasing d, the frequencies tend to the values ω_i of the isolated disks. Note also how the frequencies are dependent on the relative polarities of the disks. These results are in a quantitative agreement with micromagnetic simulations of the eigenfrequencies, showing that this method is consistent; for example, for $d = 340$ nm, from Eq. (10), we find $\omega_+^1/2\pi = 0.57$ GHz, $\omega_-^1/2\pi = 0.48$ GHz and from the simulation $\omega_+^1/2\pi = 0.57$ GHz, $\omega_-^1/2\pi = 0.51$ GHz.

C. Thiele's equation and the magnetic vortex echo

An alternative way of studying the time dependent magnetization and interaction between two magnetic nanodisks with different diameters is to use a new phenomenon, the MVE, described recently.[23] MVE is an effect of the vortex gyrotropic motion around an equilibrium position, and arises from the refocusing of the overall magnetization of the ensemble containing many nanoelements. MVE can be used as a tool to characterize nanostructures that exhibit a vortex ground state as regards the homogeneity and intensity of the interaction between its elements, properties that are relevant for device applications, as explained by Garcia *et al.*[23] In the previous work, the system studied was a matrix of nanodisks, here, we have applied the method to pairs of nanodisks.

In order to observe the MVE, one needs an ensemble of nanoelements with a distribution of gyrotropic frequencies (or distribution of diameters). In our case, we used an ensemble of 50 pairs of Permalloy nanodisks of different diameters, with constant center to center distance. We used disks with 20 nm thickness, and an approximately Gaussian distribution of diameters (average diameter of $D = 250$ nm, and $\sigma = 10$ nm); the 50 pairs were formed with disks of the same ensemble chosen in Garcia *et* al.[23]

To obtain an echo, an external magnetic field, with 25 mT intensity in the y direction, was applied to each pair of disks, displacing the vortex cores in the x direction; withdrawing the field, the cores start to process, performing a gyrotropic motion. The defocusing of the motion of the disks, due to the distribution of diameters (consequently, distribution of frequencies of width $\Delta\omega$) leads to a decay of the total magnetization $M(t)$. After a time τ, a magnetic pulse, with 300 mT intensity in the z direction and duration of 100 ps, inverts the polarity of the disks; after the pulse, the refocusing produces the MVE, as shown in Fig. 4. The decay of the total initial magnetization due to this defocusing, as well as, the decay of the echoes are characterized by a relaxation time T_2^*, which depends on the standard deviation $\Delta\omega$, on the Gilbert damping constant α and on the interaction between the neighbor disks as[23]

$$\frac{1}{T_2^*} = \Delta\omega + \frac{1}{T_2} = \Delta\omega + \frac{1}{T_2'} + \frac{1}{2T_\alpha}, \tag{11}$$

where $2T_\alpha$ is the relaxation time related to the damping constant α, and $1/T_2'$ accounts for the interaction between the disks.

Therefore, for an ensemble of disks with the same α, $1/T_2^*$ varies linearly with the strength of the interaction between them.

To obtain the vortex echo, we have used Thiele's equation to compute the coupling frequencies of the pairs of magnetic nanodisks with different diameters. The individual eigenfrequencies were computed within the two-vortex model, which is known to give more accurate results.[30] For each separation between the two disks, we computed the variation of the magnetization as a function of time; the contributions of all the 50 pairs of disks were then added. The result, after the application of the external pulse and the formation of the echo, is shown in Fig. 4(a).

The relaxation times T_2^*, that also measure the interaction strength, derived using two methods, based on the magnetic vortex echoes, are comparable, differing by about 10% (Fig. 5).

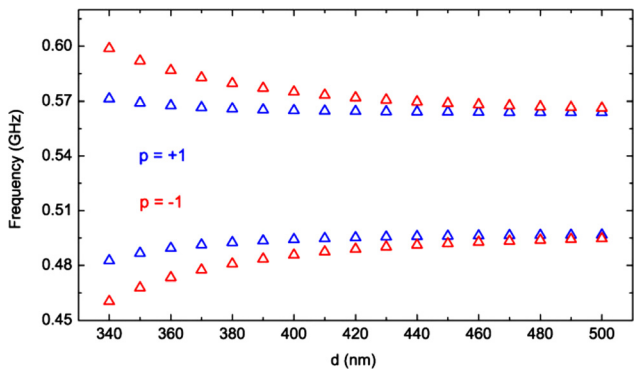

FIG. 3. Variation of coupling frequencies $\omega_\pm^p/2\pi$ with the separation distance d between two disks, with radii $R_1 = 150$ nm and $R_2 = 170$ nm, thickness 20 nm, and combined polarities $p = p_1\ p_2 = +1$ and -1. These values were obtained from Eq. (10).

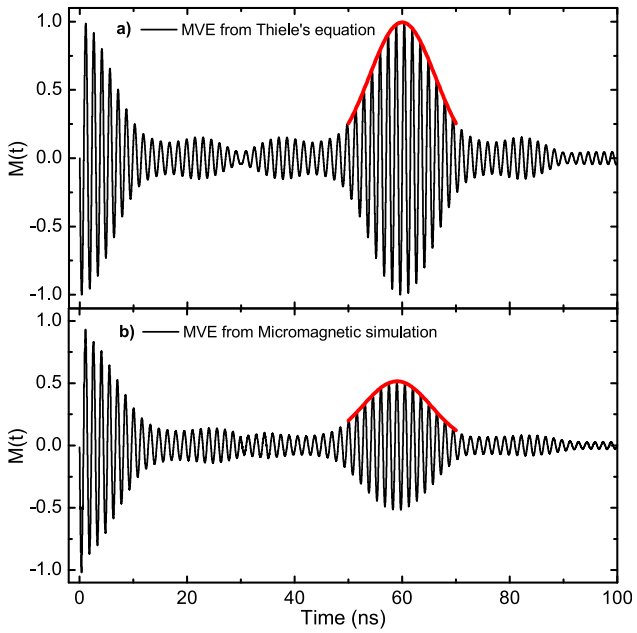

FIG. 4. Magnetization $M(t)$ of an ensemble of disk pairs separated by 450 nm, versus time, showing the initial decay and the refocalization of the rotating magnetic cores at $t = 60$ ns—the MVE. The red lines show the computer fits to the echo, used to derive the values of T_2^*. In (a) $M(t)$ was obtained by solving Thiele's equation, and in (b), $M(t)$ was obtained from a micromagnetic simulation using the OOMMF code.

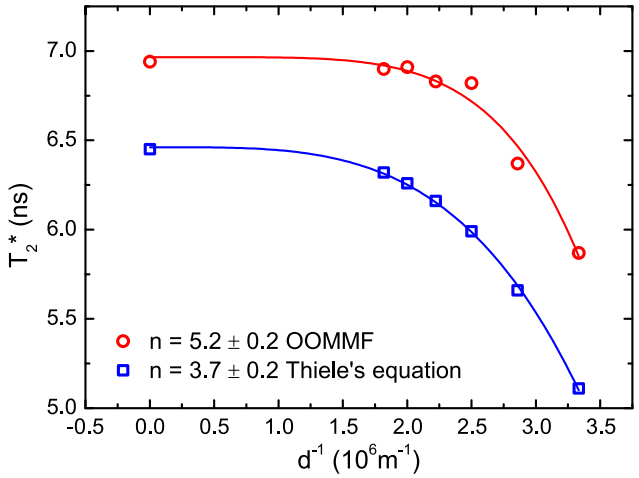

FIG. 5. Graph of T_2^* obtained from the fitting of the magnetic vortex echoes for pairs of disks with a Gaussian distribution of diameters. The continuous lines are computer fits to a function $a + b * d^{-n}$; (a) red circles represent values of T_2^* derived, for each distance, from the echoes obtained from micromagnetic simulation (fit with $n = 5.2 \pm 0.2$); (b) blue squares represent T_2^* from the echoes generated using Thiele's equation ($n = 3.7 \pm 0.2$).

D. Micromagnetic simulation and the magnetic vortex echo

The micromagnetic simulations were made for Permalloy nanodisks, cells of $5 \times 5 \times 20$ nm^3, $\alpha = 0$, using the OOMMF code.[31] Each pair of disks was simulated individually, and the overall magnetization of the 50 pairs was obtained by simply summing up the contributions of all the pairs. The echoes of the system, in which the distance between the disks was varied in the range of 260–550 nm, were then simulated.

The vortex echo obtained from the micromagnetic simulation is illustrated in Fig. 4(b); note that the echo intensity in this simulation is smaller than the magnetization at $t = 0$ ns, whereas the echo generated from Thiele's equation (Fig. 4(a)) shows no reduction in the echo intensity. This difference is associated to the energy that is transferred to the spin waves during the process of inversion of polarity in the micromagnetic simulation.

The curves of T_2^* versus disk separation were obtained from the magnetic vortex echoes and the two methods: Thiele's equation and micromagnetic simulation (Fig. 5); the results corresponding to infinite separation, were computed applying the method to individual disks.

The vortex echo analytical results are sensitive to the input eigenfrequencies. To obtain those frequencies, we used the TVA, since the rigid vortex model overestimates them with respect to the micromagnetic approach. Although the T_2^* curves obtained analytically and by micromagnetic simulation (Fig. 5) show the same qualitative behavior, a quantitative difference of about 10% is observed. This difference reflects the difference in $\Delta\omega$ observed in Sec. II B, when comparing the eigenfrequencies spread obtained analytically and from micromagnetic simulation. A larger $\Delta\omega$ means a smaller T_2^* and vice-versa, as can be seen in Eq. (11). The analytical $\Delta\omega$ is larger than the one obtained using micromagnetic simulation, and thus, the T_2^* is smaller, as observed in Fig. 5.

The difference in the values of n (of about 30%) is apparently due to the fact that, although the higher order terms of the multipolar expansion of the interaction are present in the magnetic energy used in Thiele's approach, they appear to be more relevant in the micromagnetic simulation. Another source of difference between the two results may arise from the fact that the rigid vortex model only takes into account the surface charges, whereas on the micromagnetic simulation the volume charges are also computed.

III. CONCLUSIONS

In this paper, we have studied the interaction between pairs of magnetic nanodisks of different diameters and vortex ground state; from an ensemble of magnetic nanodisks with a Gaussian distribution of diameters, we created fifty pairs of nanodisks. In this study, we have (a) derived analytically the expressions of the coupling integrals I_x and I_y that describe this interaction; (b) from the time dependent magnetizations derived from the numerical solution of Thiele's equation we applied the vortex echo method[23] to derive the dependence of the interaction with distance; (c) we made a micromagnetic simulation to obtain $M(t)$ and again applied the echo method to evaluate the strength of the interaction between the disks. We have also obtained the variation with distance between the disks, of the coupling frequencies, derived from Thiele's equation.

The coupling integrals I_x and I_y vary depending on distance in a way comparable to the results obtained by other authors. The relaxation times T_2^*, that also measure the interaction strength, derived using two methods based on the magnetic vortex echoes, are comparable, differing by about 10% (Fig. 5). The fitting to the T_2^* curves obtained from these two techniques show an approximate dependence of the form $\propto d^{-n}$, with values of n that vary between 5.2 ± 0.2 (micromagnetic simulation) and 3.7 ± 0.2 (Thiele's equation), comparable to other results of coupling between magnetic vortex disks in the literature.

ACKNOWLEDGMENTS

The authors would like to thank the support of the Brazilian agencies CNPq, FAPERJ.

[1]A. P. Guimarães, *Principles of Nanomagnetism* (Springer, Berlin, 2009).
[2]C. L. Chien, F. Q. Zhu, and J.-G. Zhu, Phys. Today **60**, 40 (2007).
[3]K. Y. Guslienko, J. Nanosci. Nanotechnol. **8**, 2745 (2008).
[4]E. R. P. Novais, P. Landeros, A. G. S. Barbosa, M. D. Martins, F. Garcia, and A. P. Guimarães, J. Appl. Phys. **110**, 053917 (2011).
[5]M. M. Soares, E. de Biasi, L. N. Coelho, M. C. dos Santos, F. S. de Menezes, M. Knobel, L. C. Sampaio, and F. Garcia, Phys. Rev. B **77**, 224405 (2008).
[6]N. A. Usov and S. E. Peschany, Phys. Met. Metall. **12**, 13 (1994).
[7]K. Y. Guslienko, V. Novosad, Y. Otani, H. Shima, and K. Fukamichi, Phys. Rev. B **65**, 024414 (2001).
[8]K. L. Metlov and K. Y. Guslienko, J. Magn. Magn. Mater. **242–245**, 1015 (2002).
[9]R. Lehndorff, D. E. Bürgler, S. Gliga, R. Hertel, P. Grünberg, C. M. Schneider, and Z. Celinski, Phys. Rev. B **80**, 054412 (2009).
[10]V. S. Pribiag, I. N. Krivorotov, G. D. Fuchs, P. M. Braganca, O. Ozatay, J. C. Sankey, D. C. Ralph, and R. A. Buhrman, Nat. Phys. **3**, 498 (2007).

[11]Q. Mistral, M. van Kampen, G. Hrkac, J.-V. Kim, T. Devolder, P. Crozat, C. Chappert, L. Lagae, and T. Schrefl, Phys. Rev. Lett. **100**, 257201 (2008).
[12]A. Dussaux, B. Georges, J. Grollier, V. Cros, A. V. Khvalkovskiy, A. Fukushima, M. Konoto, H. Kubota, K. Yakushiji, S. Yuasa, K. A. Zvezdin, K. Ando, and A. Fert, Nat. Commun. **1**, 8 (2010).
[13]S. Petit-Watelot, J.-V. Kim, A. Ruotolo, R. M. Otxoa, K. Bouzehouane, J. Grollier, A. Vansteenkiste, B. Van de Wiele, V. Cros, and T. Devolder, Nat. Phys. **8**, 682 (2012).
[14]S. Bohlens, B. Krüger, A. Drews, M. Bolte, G. Meier, and D. Pfannkuche, Appl. Phys. Lett. **93**, 142508 (2008).
[15]B. Pigeau, G. de Loubens, O. Klein, A. Riegler, F. Lochner, G. Schmidt, L. W. Molenkamp, V. S. Tiberkevich, and A. N. Slavin, Appl. Phys. Lett. **96**, 132506 (2010).
[16]H. Jung, Y.-S. Choi, K.-S. Lee, D.-S. Han, Y.-S. Yu, M.-Y. Im, P. Fischer, and S.-K. Kim, ACS Nano **6**, 3712 (2012).
[17]J. Shibata, K. Shigeto, and Y. Otani, J. Magn. Magn. Mater. **272–276**, 1688 (2004).
[18]O. V. Sukhostavets, J. González, and K. Y. Guslienko, Phys. Rev. B **87**, 094402 (2013).
[19]J. Shibata, K. Shigeto, and Y. Otani, Phys. Rev. B **67**, 224404 (2003).
[20]H. Jung, K.-S. Lee, D.-E. Jeong, Y.-S. Choi, Y.-S. Yu, D.-S. Han, A. Vogel, L. Bocklage, G. Meier, M.-Y. Im, P. Fischer, and S.-K. Kim, Sci. Rep. **1**, 59 (2011).
[21]S. Sugimoto, Y. Fukuma, S. Kasai, T. Kimura, A. Barman, and Y. C. Otani, Phys. Rev. Lett. **106**, 197203 (2011).
[22]O. V. Sukhostavets, J. M. Gonzalez, and K. Y. Guslienko, Appl. Phys. Express **4**, 065003 (2011).
[23]F. Garcia, J. P. Sinnecker, E. R. P. Novais, and A. P. Guimarães, J. Appl. Phys. **112**, 113911 (2012).
[24]D. L. Huber, Phys. Rev. B **26**, 3758 (1982).
[25]J. P. Park, P. Eames, D. M. Engebretson, J. Berezovsky, and P. A. Crowell, Phys. Rev. B **67**, 020403 (2003).
[26]H. Jung, Y.-S. Yu, K.-S. Lee, M.-Y. Im, P. Fischer, L. Bocklage, A. Vogel, M. Bolte, G. Meier, and S.-K. Kim, Appl. Phys. Lett. **97**, 222502 (2010).
[27]R. Huber and D. Grundler, Proc. SPIE **8100**, 81000D (2011).
[28]A. D. Belanovsky, N. Locatelli, P. N. Skirdkov, F. Abreu Araujo, K. A. Zvezdin, J. Grollier, V. Cros, and A. K. Zvezdin, Appl. Phys. Lett. **103**, 122405 (2013).
[29]A. Hubert and R. Schäfer, *Magnetic Domains. The Analysis of Magnetic Microstructures*, 3rd ed. (Springer, Berlin, 2009).
[30]K. Y. Guslienko, B. A. Ivanov, V. Novosad, Y. Otani, H. Shima, and K. Fukamichi, J. Appl. Phys. **91**, 8037 (2002).
[31]M. Donahue and D. Porter, OOMMF User's Guide, Version 1.0, Interagency Report No. NISTIR 6376, Technical Report, National Institute of Standards and Technology, Gaithersburg, MD, 1999.